

# Spin-entangled electrons in solid-state systems \*

Guido Burkard

*Department of Physics and Astronomy, University of Basel, Klingelbergstrasse 82,  
CH-4056 Basel, Switzerland*

Entanglement is one of the fundamental resources for quantum information processing. This is an overview on theoretical work focused on the physics of the detection, production, and transport of entangled electron spins in solid-state structures.

## Contents

<b>I. Introduction</b>	2
A. Entanglement	2
B. Electron spin entanglement	3
C. What is not covered by this review	4
<b>II. Detection of spin entanglement</b>	5
A. Localized electrons: Coupled quantum dots	5
B. Coupled dots with superconducting contacts	7
C. Mobile electrons: Beam splitter shot noise	8
D. Leads with many modes	14
E. Lower bounds for entanglement	17
F. Use of spin-orbit coupling	20
G. Backscattering	21
H. Bell's inequalities	22
<b>III. Production of spin entanglement</b>	23
A. Superconductor-normal junctions	23
B. Superconductor-Luttinger liquid junctions	25
C. Quantum dots coupled to normal leads	27

---

\* Published as: J. Phys.: Condens. Matter **19**, 233202 (2007).

D. Coulomb scattering in a 2D electron system	27
E. Other spin entangler proposals	28
<b>IV. Transport of Entangled Electrons</b>	<b>28</b>
<b>References</b>	<b>31</b>

## I. INTRODUCTION

### A. Entanglement

Entanglement is among the fundamental resources for quantum information processing. A system composed of multiple parts  $A$ ,  $B$ ,  $\dots$  is entangled if it is in a pure <sup>1</sup> state  $\psi$  that cannot be described as a tensor product  $\psi = \psi_A \otimes \psi_B \otimes \dots$ , where  $\psi_i$  denotes the wavefunction of part  $i$ . In what follows, we restrict our discussion to bipartite systems in which each of the two subsystems  $A$  and  $B$  is a single qubit for which we use spin 1/2 notation (here, we are interested in electron spin based qubit realizations). In this case, there is, up to local operations, essentially only one maximally entangled state: the spin singlet

$$|S\rangle = \frac{1}{\sqrt{2}} (|\uparrow\downarrow\rangle - |\downarrow\uparrow\rangle), \quad (1)$$

where  $|\sigma\sigma'\rangle = |\sigma\rangle \otimes |\sigma'\rangle$  and  $\sigma, \sigma' = \uparrow, \downarrow$  represent the eigenstates of the spin operator along some fixed (say,  $z$ ) direction. Note that outside the context of spin, the state Eq. (1) is also known as the *Bell state*  $|\Psi_-\rangle \equiv |S\rangle$ . The other three Bell states are (up to unimportant phases) related to  $|\Psi_-\rangle$  by the unilateral application of one of the three Pauli matrices,  $|\Psi_+\rangle = \sigma_z^{(1)}|\Psi_-\rangle$ ,  $|\Phi_-\rangle = -\sigma_x^{(1)}|\Psi_-\rangle$ , and  $|\Phi_+\rangle = \sigma_z^{(1)}|\Phi_-\rangle = -i\sigma_y|\Psi_-\rangle$ .

The notion of entanglement goes back to Erwin Schrödinger who called it the characteristic trait of quantum mechanics ([Schrödinger, 1935](#)). Schrödinger's discourse was a reaction to the famous Einstein-Podolsky-Rosen (EPR) paper ([Einstein \*et al.\*, 1935](#)) in which the non-locality of an entangled state of two remote parts had been brought forward as evidence against the completeness of quantum mechanics. As was pointed out later by John Bell, the question whether nature allows a local realistic description can be expressed in terms of an inequality for a certain combination of correlation functions and can thus be decided

---

<sup>1</sup> The definition of mixed state entanglement is somewhat more general and will be discussed further below.

experimentally if a source of entangled pairs (also called EPR pairs) like the one in Eq. (1) is available (Bell, 1966; Mermin, 1993). Such experiments have been carried out using the two linear polarizations of photons as the “qubit states” (Aspect *et al.*, 1982), providing strong evidence against local realism and for the completeness of quantum mechanics as a description of nature.

The non-locality of a system in state Eq. (1) can be viewed as a limitation since it prohibits any local description. However, from a quantum information point of view, entanglement and non-locality are “features” rather than “bugs” of quantum mechanics. This is so because entanglement between remote parties (A and B) in a quantum communications setting can be used as a resource for a variety of quantum protocols (Bennett and DiVincenzo, 2000). Among these are quantum teleportation, i.e., the faithful transmission of a quantum state using a classical channel plus previously shared entanglement (Bennett *et al.*, 1993), some variants of quantum key distribution (Ekert, 1991), i.e., the generation of an unconditionally secure cryptographic key using EPR pairs, and quantum dense coding (Bennett and Wiesner, 1992), i.e., the transmission of two classical bits by sending only one qubit and using one EPR pair. This list is by no means exhaustive: given that quantum channels can also be noisy, there exists an entire family of quantum protocols (Devetak *et al.*, 2004). In addition to the aforementioned experimental test of Bell’s inequalities (Aspect *et al.*, 1982), several quantum communication protocols have been realized experimentally with entangled photons, among them dense coding (Mattle *et al.*, 1996), quantum teleportation (Boschi *et al.*, 1998; Bouwmeester *et al.*, 1997), and quantum cryptography (Gisin *et al.*, 2002).

## B. Electron spin entanglement

The electron spin is a natural two-level system which makes it an ideal candidate for a solid-state qubit (Loss and DiVincenzo, 1998). Two electron spin qubits, each localized in one of two adjacent semiconductor quantum dots, can be coupled via the Heisenberg exchange interaction due to virtual electron tunneling between the quantum dots (Burkard *et al.*, 1999). Experimentally, there has been remarkable progress toward electron spin qubits in structures such as quantum dots: The storage, preparation, coherent manipulation of a single electron spin in a quantum dot and the controlled coupling of two spins located in separate dots has been demonstrated experimentally (Hanson *et al.*, 2006). This article is a

review of work dedicated to the question whether EPR pairs consisting of two electrons with entangled spins could be used perform those quantum protocols and to test Bell’s inequalities and in a solid-state system. Since the use of entangled electron spin pairs in solid-state structures was theoretically proposed and analyzed (Burkard *et al.*, 2000), there has been a growing activity aimed at understanding physical mechanisms that generate spin-entangled electrons in mesoscopic conductors. On the experimental side, electron spin entanglement, the violation of Bell’s inequalities, or the realization of a quantum communication protocol with electron spins in a solid have not been reported so far, but experiments are still under way in this direction. One may also envision the conversion of spin entanglement of localized (Gywat *et al.*, 2002) or mobile (Cerletti *et al.*, 2005) electrons an efficient and deterministic means to generate polarization-entangled photons.

Entanglement is not uncommon in solid-state systems. On the contrary, entanglement is the rule rather than the exception in the low-energy states (say, the ground state) of interacting many-particle systems. However, such “generic” entangled states are not necessarily useful for quantum information processing. A criterion for the usefulness as a resource is that there must be a realizable physical mechanism to extract and separate a “standard” pair of entangled particles such as the EPR pair in Eq. (1) from the many-body system in such a way that the two particles can be used for quantum communication. This is often complicated by the indistinguishability of the particles: in this case, a state that “looks entangled” when written out in first quantized notation might not be entangled in an operational sense (i.e., there may not be any physical procedure that separates the particle while maintaining their entanglement). Mathematically, this is related to the fact that the Hilbert space for several identical particles is not a tensor product when proper antisymmetrization is taken into account. Measures of entanglement which take into account the indistinguishability of particles have been introduced (Dowling *et al.*, 2006; Schliemann *et al.*, 2001a,b; Wiseman and Vaccaro, 2003).

### C. What is not covered by this review

This article is about spin entanglement between two electrons in solid-state structures. It does not cover orbital entanglement of charge carriers, such as electron-hole entanglement (see (Beenakker, 2006)), (orbital) exciton entanglement (Hohenester, 2002), orbital entangle-

ment between electrons (Samuelsson *et al.*, 2003), and entanglement between encoded spin states (Taylor *et al.*, 2005). Another review on some of the topics covered here is (Egues *et al.*, 2003).

## II. DETECTION OF SPIN ENTANGLEMENT

What physically measurable consequences does the entanglement of two electron spins in an entangled state like Eq. (1) have? How can one tell an entangled pair of electron spins (or a stream thereof) from an unentangled one? We will describe several tests for spin entanglement in this section. One of the most straight-forward methods would be to test Bell's inequality directly (in fact, such proposals have been made for electron spins in solids, as we will briefly report in Sec. II.H, further below). However, testing Bell's inequality involves measuring single electron spins one by one along at least three non-collinear quantization axes, which is by no means a simple practical task.

There is an alternative to direct Bell tests which allows to gain information about spin entanglement from a charge measurement by exploiting the Fermi statistics of the electrons, giving rise to a unique relation between the symmetry of the orbital state and the two-electron spin state. Such charge measurements can be of two different types: electrostatic (via a nearby quantum point contact or single-electron transistor) or transport (measurements of the current and/or its fluctuations).

### A. Localized electrons: Coupled quantum dots

We first consider a setup that can be used to probe the entanglement of two electrons localized in a double-dot (as shown in Fig. 1) by measuring a transport current and its fluctuations, or current noise (Loss and Sukhorukov, 2000). The parameter regime of interest is that of weak coupling between the double dot and the in- and outgoing leads (which are held at the chemical potentials  $\mu_{1,2}$ ) with tunneling amplitude  $\mathcal{T}$ , where the dots are shunted in parallel. Moreover, the parameters need to lie in (i) the Coulomb blockade regime (Kouwenhoven *et al.*, 1997) where the charge on the dots is quantized and (ii) the cotunneling regime (Averin and Nazarov, 1992), where single-electron tunneling is suppressed by energy conservation. The cotunneling regime is defined by  $U > |\mu_1 \pm \mu_2| > J > k_B T, 2\pi\nu\mathcal{T}^2$  with  $U$

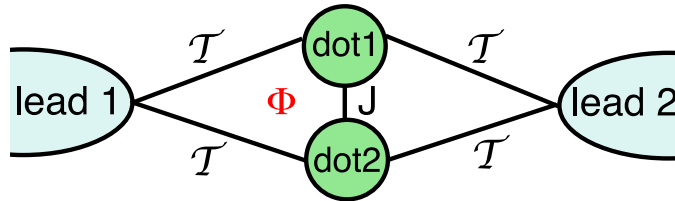


FIG. 1 Setup for detecting entanglement of two localized electrons in two tunnel-coupled quantum dots (Loss and Sukhorukov, 2000). Each dot is filled with one electron and is coupled via a tunneling amplitude  $\mathcal{T}$  to each of the two leads. In addition, the two quantum dots are tunnel-coupled amongst each other, which leads to an inter-dot exchange coupling  $J$ , energetically favoring the entangled singlet state to the triplet states of the two spins. For the detection of this entanglement, the current and/or current fluctuations from lead 1 to lead 2 need to be observed as a function of the magnetic flux  $\Phi$  threading the loop enclosed by the tunneling paths.

the charging energy on a single-dot,  $\nu$  the density of states in the leads, and  $J$  the exchange coupling between the spins on the two dots. The electric current in the cotunneling regime is generated by a coherent virtual process where one electron tunnels from one of the dots to one of the leads (say, lead 2) and then a second electron tunnels from the other lead (in our example, lead 1) to the same dot. For bias voltages exceeding the exchange coupling,  $|\mu_1 - \mu_2| > J$ , both elastic and inelastic cotunneling are permitted. It is assumed that  $\mathcal{T}$  is sufficiently small for the double-dot system to equilibrate after each tunneling event. An electron can either pass through the upper or through the lower dot, such that a closed loop is formed by these two paths. An externally applied magnetic field  $B$  then induces a magnetic flux  $\Phi = AB$  that threads this loop (with area  $A$ ) and leads to an Aharonov-Bohm (AB) phase  $\phi = e\Phi/\hbar$  between the upper and the lower path. The AB phase influences the quantum interference between the two paths. Such a transport setting is sensitive to the spin symmetry of the two-electron state on the double dot; if the two electrons on the double-dot are in the singlet state  $|S\rangle$ , as in Eq. (1), then the tunneling current acquires an additional phase of  $\pi$  leading to a sign reversal of the coherent contribution compared to

that for triplets,

$$|T_{-1}\rangle = |\downarrow\downarrow\rangle = \frac{1}{\sqrt{2}}(|\Phi_+\rangle - |\Phi_-\rangle), \quad (2)$$

$$|T_0\rangle = \frac{1}{\sqrt{2}}(|\uparrow\downarrow\rangle + |\downarrow\uparrow\rangle) = |\Psi_+\rangle, \quad (3)$$

$$|T_{+1}\rangle = |\uparrow\uparrow\rangle = \frac{1}{\sqrt{2}}(|\Phi_+\rangle + |\Phi_-\rangle). \quad (4)$$

This phase is reflected in the sign of an interference term in the average current in the cotunneling regime (Loss and Sukhorukov, 2000)

$$I = e\pi\nu^2\mathcal{T}^4 \frac{\mu_1 - \mu_2}{\mu_1\mu_2} (2 \pm \cos\phi), \quad (5)$$

where the upper (lower) sign belongs to the triplet (singlet) states in the double-dot. The fluctuations of the electric current (shot noise) follow Poissonian statistics with noise power  $S(0) = -e|I|$ , and thus they inherit the dependence on the spin state from that of the average current. Note that the singlet is maximally entangled (see above) while one of the triplets ( $|T_0\rangle$ ) is entangled (hence,  $|T_0\rangle$  is also an EPR pair) and the other two ( $|T_{\pm}\rangle$ ) are not entangled. Therefore, if the singlet can be distinguished from the triplet, then at least for one outcome (singlet), entanglement has been detected unambiguously.

For finite frequencies the shot noise is proportional to the same statistical factor (Loss and DiVincenzo, 1998),  $S(\omega) \propto (2 \pm \cos\phi)$ , where the odd part of  $S(\omega)$  leads to slowly decaying oscillations of the noise in real time,  $S(t) \propto \sin(\mu t)/\mu t$ ,  $\mu = (\mu_1 + \mu_2)/2$ . This decay is due to a charge imbalance between the two dots during a time  $\Delta t \approx \mu^{-1}$ . A general study of the quantum shot noise in cotunneling through coupled quantum dot systems can be found in (Sukhorukov *et al.*, 2001).

## B. Coupled dots with superconducting contacts

A setup similar to the one shown in Fig. 1 with two quantum dots, but connected to superconducting (SC) leads (with tunneling amplitude  $\mathcal{T}$ ), and without direct tunnel-coupling between the dots, has been considered in (Choi *et al.*, 2000). This setup is shown in Fig. 2. Two main results have been reported for this system: The coupling to the SC leads (i) energetically favors an entangled singlet-state on the dots, and (ii) provides a mechanism for detecting the spin state via the Josephson current through the double dot system.

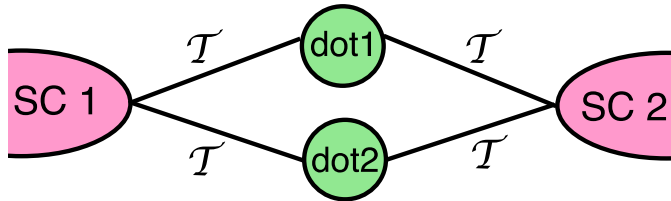


FIG. 2 The setup described in (Choi *et al.*, 2000): Two quantum dots are connected in a parallel shunt between two SC contacts (tunneling amplitude  $\mathcal{T}$ ), without any direct tunnel coupling between the quantum dots.

The lowest-order tunneling effects  $\propto \mathcal{T}^4$  are captured with the following Heisenberg spin Hamiltonian (Choi *et al.*, 2000),

$$H_{\text{eff}} \approx J \left( 1 + \cos \varphi \right) \left( \mathbf{S}_1 \cdot \mathbf{S}_2 - \frac{1}{4} \right), \quad (6)$$

with an exchange coupling  $J \approx 2\mathcal{T}^2/\epsilon$ , where  $\epsilon$  is the energy separation between the quantum dot state and the Fermi level, and  $\varphi$  is the average phase difference between the two SC reservoirs. The exchange coupling  $J$  can be controlled by tuning the external parameters  $\mathcal{T}$  and  $\varphi$ , thus providing an implementation of an entangler (see Sec. III below). The two-spin state (singlet or triplet) on the double dot can be probed with a transport measurement by forming a SQUID with the device shown in Fig. 2 combined in a parallel shunt with one additional (ordinary) Josephson junction with coupling  $J'$  and phase difference  $\theta$ . The SC current  $I_S$  in such a ring circuit is then found to be (Choi *et al.*, 2000)

$$I_S/I_J = \begin{cases} \sin(\theta - 2\pi\phi/\phi_0) + (J'/J) \sin \theta, & \text{singlet,} \\ (J'/J) \sin \theta, & \text{triplets,} \end{cases} \quad (7)$$

where  $I_J = 2eJ/\hbar$ ,  $\phi$  is the magnetic flux threading the SQUID loop, and  $\phi_0$  the SC flux quantum. By ramping a dc current  $I$  through the ring until the SC switches to its normal state at  $|I| > I_c$  and a finite voltage  $V$  appears, the spin- and flux-dependent critical current  $I_c = \max_{\theta}\{|I_S|\}$  can be determined.

### C. Mobile electrons: Beam splitter shot noise

In the preceding Sec. II.A, we have discussed the detection of entanglement in the ground state of two electrons *localized* in a double-dot structure via the electric current and noise across the structure. Now, we turn to the detection of spin entanglement of *mobile* electron



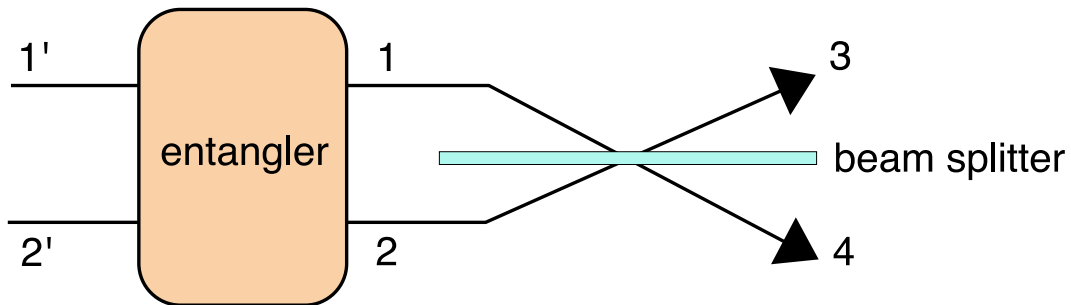


FIG. 3 The beam-splitter setup. An entangler (see Sec. III) transforms uncorrelated electrons (here schematically indicated as leads 1' and 2') into pairs of electrons in the entangled singlet (triplet) state  $|\Psi_{\mp}\rangle$ , which are injected into leads 1, 2 (one electron per lead). The entanglement of the spin singlet can then be detected in an interference measurement with the beam splitter: Since the orbital wave function of the singlet is symmetric, the electrons leave the scattering region preferably in the same lead (3 or 4), cf. Table I. This correlation of the particle number (“bunching”) manifests itself in an enhancement of the shot noise by a factor of 2 in the outgoing leads.

spins. For this purpose, the electron pair to be tested will itself carry the electric current. It turns out that pairwise spin entanglement between electrons in two mesoscopic conductors can be detected in the fluctuations of the charge current after transmission through an electronic beam splitter (Burkard *et al.*, 2000) as shown schematically in Fig. 3. As we discuss in detail below, the singlet EPR pair Eq. (1) produces an enhancement of the shot noise power (“bunching” behavior), whereas the triplets  $|T_{0,\pm 1}\rangle$ , Eqs. (2–4) lead to a suppression of noise (“antibunching”).

This result can be understood by inspection of Table I. For indistinguishable, Fermionic particles such as electrons, the antisymmetry of the total wavefunction (spin and orbit combined) dictates that the orbital wavefunction must be symmetric if the spin wavefunction is antisymmetric (as in the case of the spin singlet) and vice versa for the triplets. Assuming

state	spin wavefunction	orbital wavefunction	final states (orbit)	$\langle \delta N_3^2 \rangle$	entanglement
$ S\rangle$	antisymmetric	symmetric	$ 33\rangle,  44\rangle$	1	yes
$ T_0\rangle$	symmetric	antisymmetric	$ 34\rangle -  43\rangle$	0	yes
$ T_{\pm}\rangle$	symmetric	antisymmetric	$ 34\rangle -  43\rangle$	0	no
distinguishable	—	—	$ 33\rangle,  44\rangle,  34\rangle,  43\rangle$	1/2	possible

TABLE I Number statistics for Fermions at a symmetric beam splitter.

that each conductor has only one channel (which we simply denote  $|n\rangle$  where  $n$  is the label of the contact), we can easily enumerate all possible final states with the prescribed symmetry. The task of the beam splitter is to distribute the particles over these possible states in order to probe the symmetry properties of the wavefunction. For a symmetric beam splitter where the transmission and reflection probabilities are both  $1/2$  (for the general case, see below), each of these states allowed by symmetry is filled with equal probability. Then, it is easy to obtain the mean and variance of the probability distribution for  $N = N_3$ , the number of outgoing electrons in lead  $n = 3$  (Loudon, 1998). The mean is always  $\langle N \rangle = 1$  and does not contain any information on the statistics or entanglement of the ingoing state. We therefore do not expect that here (unlike for the localized electrons in Sec. II.A), the average electric current will contain any information about the spin state. However, the variance  $\langle \delta N_3^2 \rangle$  vanishes for triplets because there is only one possible final state and thus fluctuations are impossible (this behavior is called “antibunching” of particles), while for the singlet  $\langle \delta N_3^2 \rangle = 1$  which is twice as large as expected for (classical) distinguishable particles (also known as “bunching”). Note that for Bosons (e.g., photons), since the total wavefunction must be symmetric, the role of singlet and triplet are interchanged. In fact, for Bosons, this effect is well known as the Hong-Ou-Mandel dip in interferometry with entangled photon pairs (Hong *et al.*, 1987). Bunching behavior for (unentangled) Bosons also underlies the famous Hanbury-Brown and Twiss experiment (Hanbury Brown and Twiss, 1956).

Here, we are interested in the fact that particle bunching, i.e., the enhancement of the fluctuations of the electron current, is only possible for an entangled state (the singlet) and thus particle bunching is a unique signature for entanglement. Nothing of this sort can be said for antibunching, since there are both entangled and unentangled triplets. This result can be extended to non-maximally entangled states (see below for a quantitative discussion); we only anticipate here that in Table I, we find  $\langle \delta N_3^2 \rangle \leq 1/2$  for all unentangled states. Conversely, a number fluctuation  $\langle \delta N_3^2 \rangle > 1/2$  can be interpreted as a signature of entanglement. However, we still need to relate  $\langle \delta N_3^2 \rangle$  to a physically measurable quantity (the shot noise power at low frequencies).

Let us now turn to the physical setup (Fig. 3) with a beam splitter where electrons have an amplitude  $t$  to be interchanged (without mutual interaction) such that  $0 < |t|^2 < 1$ . Shot noise of the electric current in such beam splitter devices have been studied for normal (unentangled) electrons both in theory (Büttiker, 1990, 1992; Martin and Landauer,

1992; Torrès and Martin, 1999) and experiment (Henny *et al.*, 1999; Liu *et al.*, 1998; Oliver *et al.*, 1999). Recent experiments have investigated the sign of the cross-correlations after transmission of fermions through a beam splitter and the distinction between the effects from Fermi statistics and other effects such as noisy injection and interactions (Chen and Webb, 2006; Oberholzer *et al.*, 2006). These experiments have been performed in semiconductor nanostructures with geometries that are very similar to the set-up proposed in Fig. 3 but without any entangler device.

The effect of interactions in the leads will be addressed in Sec. IV below. To calculate the shot noise of spin-entangled electrons, standard scattering theory (Blanter and Büttiker, 2000; Büttiker, 1990, 1992), was extended to a situation with entanglement (Burkard *et al.*, 2000). The entangled two-electron state injected into two distinct leads 1 and 2 can be written in second quantized notation as

$$|\Psi_{\pm}\rangle \equiv |\psi_{\mathbf{n}\mathbf{n}'}^{t/s}\rangle = \frac{1}{\sqrt{2}} (a_{\mathbf{n}\uparrow}^{\dagger} a_{\mathbf{n}'\downarrow}^{\dagger} \pm a_{\mathbf{n}\downarrow}^{\dagger} a_{\mathbf{n}'\uparrow}^{\dagger}) |\psi_0\rangle, \quad (8)$$

where  $s$  and  $t$  stand for the singlet and triplet,  $|\psi_0\rangle$  for the filled Fermi sea, and  $\mathbf{n} = (\mathbf{q}, l)$ , where  $\mathbf{q}$  denotes the momentum and  $l$  the lead quantum number of an electron. The operator  $a_{\mathbf{n}\sigma}^{\dagger}$  creates an electron in state  $\mathbf{n}$  with spin  $\sigma$ . Alternatively, we can use the quantum numbers  $\mathbf{n} = (\varepsilon_n, n)$ , with the electron energy  $\varepsilon_n$  instead of the momentum as the orbital quantum number in Eq. (8). The operator  $a_{\alpha\sigma}^{\dagger}(\varepsilon)$  then creates an incoming electron in lead  $\alpha$  with spin  $\sigma$  and energy  $\varepsilon$ . After being injected, the two electrons are no longer distinguishable from the electrons that had been in the leads before, and consequently the two electrons retrieved from the system will, in general, not be “the same” as the ones injected. When extending the theory for the current correlations in a multiterminal conductor (Büttiker, 1990, 1992) to the case of entangled scattering states, we need to take into account that Wick’s theorem cannot be applied anymore. The current operator for lead  $\alpha$  of a multiterminal conductor is

$$I_{\alpha}(t) = \frac{e}{h\nu} \sum_{\varepsilon\varepsilon'\sigma} [a_{\alpha\sigma}^{\dagger}(\varepsilon)a_{\alpha\sigma}(\varepsilon') - b_{\alpha\sigma}^{\dagger}(\varepsilon)b_{\alpha\sigma}(\varepsilon')] \exp[i(\varepsilon - \varepsilon')t/\hbar], \quad (9)$$

with the operators  $b_{\alpha\sigma}(\varepsilon)$  for the outgoing electrons, that are related to the operators  $a_{\alpha\sigma}(\varepsilon)$  for the incident electrons via  $b_{\alpha\sigma}(\varepsilon) = \sum_{\beta} s_{\alpha\beta} a_{\beta\sigma}(\varepsilon)$ , where  $s_{\alpha\beta}$  is the scattering matrix. Here, the scattering matrix is assumed to be spin- and energy-independent. For a discrete energy spectrum in the leads, the operators  $a_{\alpha\sigma}(\varepsilon)$  can be normalized such that

$\{a_{\alpha\sigma}(\varepsilon), a_{\beta\sigma'}^\dagger(\varepsilon')\} = \delta_{\sigma\sigma'}\delta_{\alpha\beta}\delta_{\varepsilon\varepsilon'}/\nu$ , where the Kronecker symbol  $\delta_{\varepsilon\varepsilon'}$  equals 1 if  $\varepsilon = \varepsilon'$  and 0 otherwise and where  $\nu$  denotes the density of states in the leads. As mentioned before, we assume for the moment that each lead consists of only a single quantum channel, a more general treatment will be discussed in Sec. II.D below. The current operator Eq. (9) can now be written in terms of the scattering matrix as

$$I_\alpha(t) = \frac{e}{h\nu} \sum_{\varepsilon\varepsilon'\sigma} \sum_{\beta\gamma} a_{\beta\sigma}^\dagger(\varepsilon) A_{\beta\gamma}^\alpha a_{\gamma\sigma}(\varepsilon') e^{i(\varepsilon-\varepsilon')t/\hbar}, \quad (10)$$

$$A_{\beta\gamma}^\alpha = \delta_{\alpha\beta}\delta_{\alpha\gamma} - s_{\alpha\beta}^* s_{\alpha\gamma}. \quad (11)$$

The current-current correlator between  $I_\alpha(t)$  and  $I_\beta(t)$  in two leads  $\alpha, \beta = 1, \dots, 4$  of the beam splitter is then

$$S_{\alpha\beta}^\chi(\omega) = \lim_{\tau \rightarrow \infty} \frac{h\nu}{\tau} \int_0^\tau dt e^{i\omega t} \text{Re Tr} [\delta I_\alpha(t) \delta I_\beta(0) \chi], \quad (12)$$

where  $\delta I_\alpha = I_\alpha - \langle I_\alpha \rangle$ ,  $\langle I_\alpha \rangle = \text{Tr}(I_\alpha \chi)$  and  $\chi$  is the density matrix of the injected electron pair. Here, we are interested in the zero-frequency correlator  $S_{\alpha\beta} \equiv S_{\alpha\beta}^\chi(0)$ . In order not to overburden our notation, we omit the dependence on  $\chi$  in what follows. If we substitute  $\chi = |\Psi_\pm\rangle\langle\Psi_\pm|$  we obtain

$$S_{\alpha\beta} = \frac{e^2}{h\nu} \left[ \sum_{\gamma\delta}' A_{\gamma\delta}^\alpha A_{\delta\gamma}^\beta \mp \delta_{\varepsilon_1, \varepsilon_2} (A_{12}^\alpha A_{21}^\beta + A_{21}^\alpha A_{12}^\beta) \right], \quad (13)$$

where  $\sum_{\gamma\delta}'$  denotes the sum over  $\gamma = 1, 2$  and all  $\delta \neq \gamma$ , and the upper (lower) sign refers again to triplets (singlets). Physically, the autocorrelator  $S_{\alpha\alpha}$  is the shot noise measured in lead  $\alpha$ .

The formula Eq. (13) can now be applied to the setting shown in Fig. 3, i.e., involving four leads and described by the single-particle scattering matrix elements,  $s_{31} = s_{42} = r$ , and  $s_{41} = s_{32} = t$ , where  $r$  and  $t$  denote the reflection and transmission amplitudes at the beam splitter. If we neglect backscattering (see Sec. II.G for a discussion of the influence of backscattering), i.e.,  $s_{12} = s_{34} = s_{\alpha\alpha} = 0$ , then the noise correlations for the incident state  $|\Psi_\pm\rangle$  are found to be (Burkard *et al.*, 2000)

$$S_{33} = S_{44} = -S_{34} = 2 \frac{e^2}{h\nu} T (1 - T) (1 \mp \delta_{\varepsilon_1 \varepsilon_2}), \quad (14)$$

with  $T = |t|^2$  the transmittivity of the beam splitter. One can check that for the remaining two triplet states  $|\uparrow\uparrow\rangle$  and  $|\downarrow\downarrow\rangle$  one also obtains Eq. (14) with the upper sign. As anticipated,

the average current in all leads is a constant, both for singlets and triplets,  $|\langle I_\alpha \rangle| = e/h\nu$ . The shot noise power is often expressed in terms of the noise-to-current ratio (or, more accurately, the ratio between the actual noise power and that of a Poissonian source (Blanter and Büttiker, 2000)), the so-called Fano factor,  $F = S_{\alpha\alpha}/2e|\langle I_\alpha \rangle|$ . In our case, the theoretical prediction for the Fano factor is (note the absence of a factor of  $2e$  with the above definition of the Fano factor),

$$F = T(1 - T)(1 \mp \delta_{\varepsilon_1\varepsilon_2}). \quad (15)$$

The formula Eq. (15) implies that if electrons in the singlet state  $|\Psi_-\rangle$  with equal energies,  $\varepsilon_1 = \varepsilon_2$ , i.e., in the same orbital mode, are injected pairwise into the leads 1 and 2, then the zero frequency noise is *enhanced* by a factor of two (Burkard *et al.*, 2000),  $F = 2T(1 - T)$ , with respect to the noise power for unentangled (uncorrelated) electrons (Büttiker, 1990, 1992; Khlus, 1987; Landauer, 1989; Lesovik, 1989; Martin and Landauer, 1992),  $F = T(1 - T)$ . As explained above, this noise enhancement is due to *bunching* of electrons in the outgoing leads, caused by the symmetric orbital wavefunction of the spin singlet  $|S\rangle = |\Psi_-\rangle$ . The triplet states  $|T_0\rangle = |\Psi_+\rangle$ ,  $|\uparrow\uparrow\rangle$ , and  $|\downarrow\downarrow\rangle$  exhibit *antibunching*, i.e. a complete suppression of the noise,  $S_{\alpha\alpha} = 0$ . The noise enhancement for the singlet  $|\Psi_-\rangle$  is therefore a unique signature for entanglement (no unentangled state exists which can lead to the same signal). Entanglement can thus be observed by measuring the noise power of a mesoscopic conductor in a setup like Fig. 3. Distinguishing the triplet states  $|\Psi_+\rangle$ ,  $|\uparrow\uparrow\rangle$ , and  $|\downarrow\downarrow\rangle$  is not possible with the described noise measurement alone; their discrimination requires a measurement of the spins of the outgoing electrons, e.g. by using spin-selective tunneling devices (Prinz, 1998) into leads 3 and 4. However, as we shall discuss in Sec. II.F below, there are ways to detect triplet entanglement if a local spin rotation mechanism (e.g., provided by the spin-orbit interaction) is available in at least one of the ingoing leads.

Signatures of entanglement in the charge transport statistics have also been formulated in the framework of the full counting statistics (Börlin *et al.*, 2002; Di Lorenzo and Nazarov, 2005; Faoro *et al.*, 2004; Taddei *et al.*, 2005; Taddei and Fazio, 2002). The generalization (for both Bosons and Fermions) to many particles interfering at a multi-port beam splitter is discussed in (Lim and Beige, 2005).

### D. Leads with many modes

In our discussion so far, we have assumed that the leads that carry the spin-entangled electrons from the entangler to the beam splitter only conduct electrons via a single quantized mode. This has been extended to the continuum limit for the lead spectrum in (Samuelsson *et al.*, 2004). We will follow a somewhat more general discussion (including the continuum case) for leads with multiple modes as presented in (Egues *et al.*, 2005). In this general discussion, the parameter regimes in which singlet spin entanglement can be detected in the shot noise at a beam splitter (as discussed in Sec. II.C above) have been identified. It turns out that even in the case where the entangled electrons are injected into a multitude of discrete states of the lead, we can observe two-particle coherence, and thus particle bunching and antibunching, and thus detect entangled states. In our discussion, we are not considering the possibility that in a multi-mode setting, the two injected electrons can also be entangled in their orbital degrees of freedom. This possibility and its consequences for the entanglement detection via a noise measurement at a beam splitter has been investigated in (Giovannetti *et al.*, 2006).

For our purposes, we first identify the relevant energy scales for the transport through multiple modes. These are the level spacing  $\delta$  in the leads, the energy mismatch  $\Delta$  of the injected electrons, and the energy broadening  $\gamma$  of the injected electrons (see Fig. 4). The relative magnitude of these three energies determine six different parameter regimes. In four of the six regimes, the full two-particle interference (and thus detection of spin entanglement) can be achieved asymptotically. In the two remaining parameter regimes, characterized by  $\Delta \gg \delta, \gamma$ , i.e., the energy mismatch exceeding both the level spacing and the energy broadening, we obtain no two-particle interference (these represent two distinct parameter regimes, since  $\delta$  can be smaller or larger than  $\gamma$ ).

The lead spectrum is assumed to consist of equidistant levels, i.e.,  $\varepsilon_n = n\delta + q\delta$ , where  $n = 0, \pm 1, \pm 2, \dots$  and  $0 \leq q < 1$  is some fixed offset. The injection of an electron with spin  $\sigma = \uparrow, \downarrow$  into the lead  $\alpha$  with energy distribution  $g(\varepsilon, \varepsilon_n)$  centered at  $\varepsilon_n$  is now described by the creation operator

$$c_{\alpha\sigma}^\dagger(\varepsilon) = \sum_{n=-\infty}^{\infty} g(\varepsilon, \varepsilon_n) a_{\alpha\sigma}^\dagger(\varepsilon_n), \quad (16)$$

where  $a_{\alpha\sigma}^\dagger(\varepsilon_n)$  creates an electron with the sharp energy  $\varepsilon_n$  as in Eq. (8). For the weight

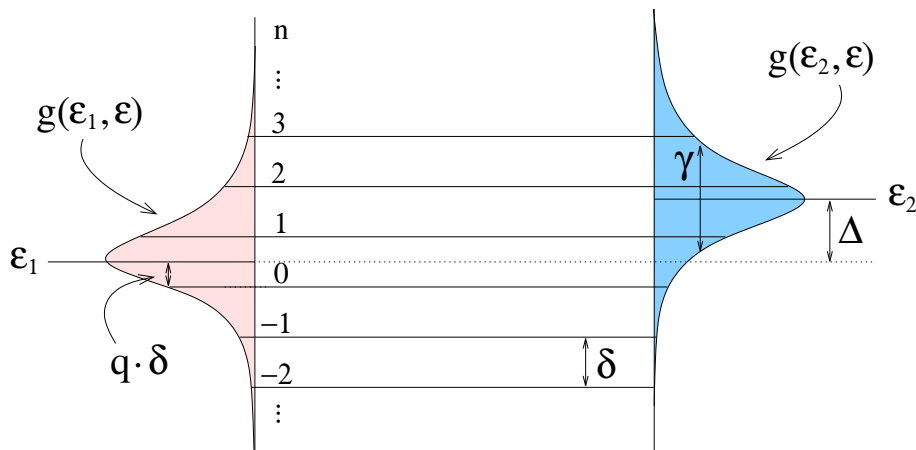


FIG. 4 Energy diagram for the injection of entangled electrons into leads with multiple levels (Egues *et al.*, 2005). In the model discussed in the main text, the energy levels in the leads  $n = 0, \pm 1, \pm 2, \dots$  are assumed to be equidistant with spacing  $\delta$ . The injection of electrons takes place at the mean energies  $\varepsilon_{1,2}$  (for electron 1 and 2, respectively), separated by  $\Delta = \varepsilon_2 - \varepsilon_1$ , and with distributions  $g(\varepsilon_{1,2}, \varepsilon)$  of width  $\gamma$ . Here, the distributions  $g(\varepsilon_{1,2}, \varepsilon)$  are not drawn to scale, since their normalizations depend on the value of  $q$ .

function  $g$ , we use the Breit-Wigner form

$$g(\varepsilon, \varepsilon') = \frac{g_0(\varepsilon)}{\varepsilon - \varepsilon' + i\gamma}, \quad (17)$$

subject to the normalization condition  $\sum_{n=-\infty}^{\infty} |g(\varepsilon, \varepsilon')|^2 = 1$ .

Here, we assume that the entangler injects an electron with total probability 1, but with uncertain energy (e.g., using time-dependent tunnel barriers). This is different from the weak tunneling case, e.g., from a quantum dot (Recher *et al.*, 2001). Analogous to Eq. (8), the spin-entangled singlet ( $-$ ) and triplet ( $+$ ) states for many-mode leads can be written with the new creation operators as

$$|\Psi_{\pm}\rangle = \frac{1}{\sqrt{2}} \left( c_{1\uparrow}^{\dagger}(\varepsilon_1) c_{2\downarrow}^{\dagger}(\varepsilon_2) \pm c_{1\downarrow}^{\dagger}(\varepsilon_1) c_{2\uparrow}^{\dagger}(\varepsilon_2) \right) |\psi_0\rangle. \quad (18)$$

The relation Eq. (16) allows us to express these states as

$$|\Psi_{\pm}\rangle = \sum_{\varepsilon'_1, \varepsilon'_2} g(\varepsilon_1, \varepsilon'_1) g(\varepsilon_2, \varepsilon'_2) |\Psi_{\pm}\rangle_{\varepsilon'_1, \varepsilon'_2}, \quad (19)$$

where  $|\Psi_{\pm}\rangle_{\varepsilon'_1, \varepsilon'_2}$  are the states with sharp energies, defined in Eq. (8). The normalization condition for  $g(\varepsilon_1, \varepsilon'_1)$  ensures that the average current in the outgoing leads of the beam

splitter is unaffected by the spread in energy, i.e.,  $I_3 = I_4 = -e/h\nu$ . However, the Fano factor  $F = S_{33}/2eI_3$  does depend on the energy distribution,

$$F = T(1 - T) (1 \mp |h(\varepsilon_1, \varepsilon_2)|^2), \quad (20)$$

where the upper (lower) sign corresponds to the entangled triplet (singlet), and where the overlap function  $h$  is defined as

$$h(\varepsilon_1, \varepsilon_2) = \sum_{\varepsilon} g(\varepsilon_2, \varepsilon)^* g(\varepsilon_1, \varepsilon). \quad (21)$$

For equidistant levels, this function has been evaluated exactly (note that the  $q$  dependence has dropped out),

$$|h|^2 = \frac{\gamma^2}{(\Delta/2)^2 + \gamma^2} \frac{\cosh^2(2\pi\gamma/\delta) - \cos^2(\pi\Delta/\delta)}{\sinh^2(2\pi\gamma/\delta)}. \quad (22)$$

In the case of injection into a single level, the  $|h|^2$  term that appears in Eq. (20) for the Fano factor reduces to a Kronecker delta, as in Eq. (15). The role of the function  $0 < |h(\Delta, \delta, \gamma)|^2 \leq 1$  is to quantify the visibility of two-particle interference. We plot the dimensionless quantity  $|h(\Delta, \delta, \gamma)|^2$  as a function of the dimensionless ratios  $\Delta/\delta$  and  $\delta/\gamma$  in Fig. 5. For maximal visibility,  $|h|^2 = 1$ , full bunching and antibunching of singlets and entangled triplets can be expected; this is the ideal case with regards to the detection of entanglement. In the opposite case  $|h|^2 = 0$ , bunching or antibunching cannot be observed at all because the two wave packets centered around  $\varepsilon_1$  and  $\varepsilon_2$  do not overlap in energy.

We briefly highlight the main parameter regimes (see also Fig. 5). (1) If the two electrons are injected with energy distributions whose centers coincide,  $\Delta = \varepsilon_1 - \varepsilon_2 = 0$ , then the interference is always maximal,  $|h|^2 = 1$ , irrespective of the values of the parameters  $\delta$  and  $\gamma$ . For finite but small  $\Delta$ , i.e.,  $\Delta \ll \gamma, \delta$ , one finds  $|h|^2 = 1 - O(\Delta^2)$ . More precisely, for  $\Delta \ll \gamma \ll \delta$ , the correction is  $|h|^2 \simeq 1 - \pi^2\Delta^2/3\delta^2$ , whereas for  $\Delta \ll \delta \ll \gamma$ , one finds  $|h|^2 \simeq 1 - \Delta^2/4\gamma^2$ . (2) If the energy broadening is small,  $\gamma \ll \delta, \Delta$ , then Eq. (22) yields

$$|h|^2 = \frac{\delta^2}{\pi^2\Delta^2} \sin^2 \pi \frac{\Delta}{\delta} + O(\gamma^2). \quad (23)$$

Here, the ratio  $\delta/\Delta$  is essential: If  $\gamma \ll \delta \ll \Delta$  then the two electrons are injected into two different discrete states, therefore  $|h|^2 \rightarrow 0$ . In the opposite limit,  $\gamma \ll \Delta \ll \delta$ , the two electrons are injected into the same discrete level and  $|h|^2 = 1 - \pi^2\Delta^2/3\delta^2 + O(\Delta^4/\delta^4, \gamma^2)$ .



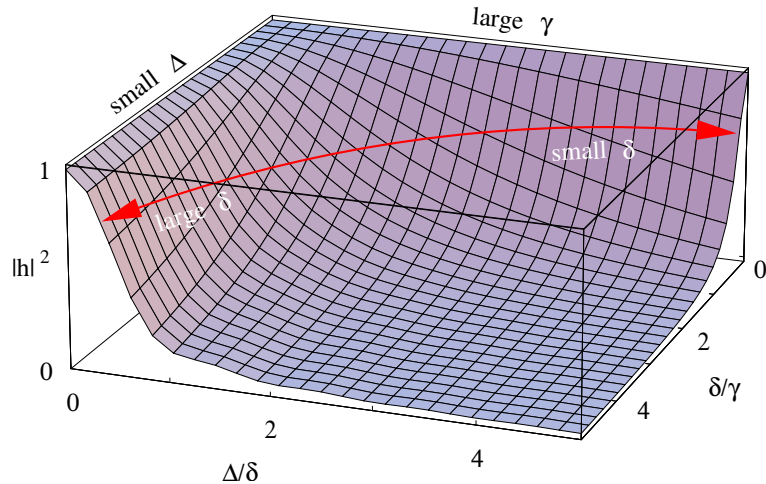


FIG. 5 The two-particle interference visibility  $|h(\Delta, \delta, \gamma)|^2$  from Eq. (22), plotted as a function of the dimensionless quantities  $\Delta/\delta$  and  $\delta/\gamma$ , where  $\Delta = \varepsilon_2 - \varepsilon_1$  denotes the mean energy difference between the two injected electrons,  $\gamma$  the width of their energy distributions, and  $\delta$  the level spacing in the leads (see Fig. 4). The special case of matching energies  $\varepsilon_1 \approx \varepsilon_2$  or  $\Delta \ll \delta, \gamma$  corresponds to the edge labeled by “small  $\Delta$ ”; here we find  $|h|^2 = 1$ , irrespective of the ratio  $\gamma/\delta$ . The case of a broad energy distribution (fast injection)  $\gamma \gg \Delta, \delta$  corresponds to the edge labeled “large  $\gamma$ ”; along this edge  $|h|^2 = 1$ , regardless of  $\Delta/\delta$ . A line of constant  $\gamma$  and  $\Delta$  with variable  $\delta$  is indicated by a red arrow. For large  $\delta$ , we find again  $|h|^2 = 1$  for all  $\Delta/\gamma$ , whereas for small  $\delta$  (continuum limit), the limit  $|h|^2 = 0$  or  $|h|^2 = 1$  is reached, depending on whether  $\Delta/\gamma \gg 1$  or  $\Delta/\gamma \ll 1$ .

(3) The continuum limit is reached when  $\delta \ll \Delta, \gamma$ . In this case  $|h|^2$  has the shape of a Lorentzian (Samuelsson *et al.*, 2004),

$$|h|^2 \simeq \frac{\gamma^2}{(\Delta/2)^2 + \gamma^2}. \quad (24)$$

Depending on the ratio  $\gamma/\Delta$ , the two-particle interference is present or absent, i.e.,  $|h|^2 \rightarrow 0$  for  $\delta \ll \gamma \ll \Delta$ , while  $|h|^2 \rightarrow 1$  for  $\delta \ll \Delta \ll \gamma$ . In summary, highly visible two-particle interference (and thus bunching and antibunching)  $|h|^2 \rightarrow 1$  can be expected in all asymptotic regimes except for the detuned cases,  $\Delta \gg \delta, \gamma$ , where  $|h|^2 \rightarrow 0$ .

### E. Lower bounds for entanglement

In Sec. II.C above, the current fluctuations for a maximally entangled state (the singlet) has been discussed. Here, we extend this analysis to non-maximally entangled states. Such

states can be both pure or mixed, and therefore are generally described by a density matrix  $\chi$ . It turns out (Burkard and Loss, 2003) that using the zero-frequency noise amplitude after passage through the beam splitter (Fig. 6), one can determine a *lower bound* for the *amount*  $E$  of spin entanglement carried by individual pairs of electrons. One can therefore relate experimentally accessible quantities with a standard measure for entanglement, the entanglement of formation  $E$  (Bennett *et al.*, 1996b). Such knowledge is important since  $E$  quantifies the usefulness of a bipartite state for quantum communication.

We start our discussion from a general mixed state which we write in the singlet-triplet basis,

$$\chi = F_S |\Psi_-\rangle \langle \Psi_-| + G_0 |\Psi_+\rangle \langle \Psi_+| + \sum_{i=\uparrow, \downarrow} G_i |ii\rangle \langle ii| + \Delta\chi, \quad (25)$$

where  $\Delta\chi$  denote off-diagonal terms. The singlet fidelity  $F_S$  quantifies the probability that the electron pair is in a spin singlet state (we use the subscript  $S$  here in order to distinguish the singlet fidelity from the Fano factor; in the literature,  $F$  is often used for  $F_S$ ). Next, one can decompose the current correlators Eq. (12) as

$$S_{\alpha\beta} \equiv S_{\alpha\beta}^\chi = F_S S_{\alpha\beta}^{|\Psi_-\rangle} + G_0 S_{\alpha\beta}^{|\Psi_+\rangle} + \sum_{i=\uparrow, \downarrow} G_i S_{\alpha\beta}^{ii}, \quad (26)$$

where we have defined  $S_{\alpha\beta}^{|\Psi\rangle} \equiv S_{\alpha\beta}^{|\Psi\rangle \langle \Psi|}$ . The off-diagonal terms in  $\Delta\chi$  need not be specified further, as they do not enter  $S_{\alpha\beta}$  due to the spin-conserving nature of the operators  $\delta I_\alpha(t)$ . The prefactors  $F_S$ ,  $G_0$ ,  $G_\uparrow$ , and  $G_\downarrow$  are the diagonal matrix elements of  $\chi$  and are determined by the state preparation, i.e., the entangler.

In Sec. II.C we showed that the singlet state  $|S\rangle = |\Psi_-\rangle$  gives rise to enhanced shot noise (and cross-correlators),  $S_{33}^{|\Psi_-\rangle} = -S_{34}^{|\Psi_-\rangle} = 2eIT(1-T)f$ , with the *reduced correlator*  $f = 2$ , as compared to the ‘‘classical’’ Poissonian value  $f = 1$ . The spin triplet states, on the other hand, are noiseless,  $S_{\alpha\beta}^{|\Psi_+\rangle} = S_{\alpha\beta}^{|\uparrow\uparrow\rangle} = S_{\alpha\beta}^{|\downarrow\downarrow\rangle} = 0$  ( $\alpha, \beta = 3, 4$ ). Therefore, both the auto- and cross-correlations are only due to the singlet component of the incident two-particle state,

$$S_{33} = -S_{34} = F_S S^{|\Psi_-\rangle} = 2eIT(1-T)f, \quad (27)$$

where  $f = 2F_S$ . So, a noise measurement simply provides us with the information about the singlet fraction of the state. This already suggests that in general, we cannot expect to get full information about the entanglement  $E$  of the state, since  $E$  is a function of the entire density matrix  $\chi$  of which we know only one matrix element! From this point of view it is

astonishing how much we can know about the entanglement  $E$  by knowing only  $F_S$ : as we explain below, we can always obtain a lower bound on  $E$  which becomes tight if the state is a singlet ( $F_S = 1$ ,  $E = 1$ ) or any other spherically symmetric state.

Given a *pure* bipartite state,  $|\psi\rangle \in \mathcal{H}_A \otimes \mathcal{H}_B$ , we can use the von Neumann entropy  $S_N(|\psi\rangle) = -\text{Tr}_B \rho_B \log \rho_B$  (log in base 2) of the reduced density matrix  $\rho_B = \text{Tr}_A |\psi\rangle\langle\psi|$ , to quantify the entanglement. This quantity is always between 0 and 1,  $0 \leq S_N \leq 1$ , and is maximal for the Bell states,  $S_N(|\Psi_{\pm}\rangle) = S_N(|\Phi_{\pm}\rangle) = 1$ . If it vanishes, then the state is unentangled (i.e., a tensor product state),  $S_N(|\psi\rangle) = 0 \Leftrightarrow |\psi\rangle = |\psi\rangle_A \otimes |\psi\rangle_B$ . The operational meaning is that if  $S_N(|\psi\rangle) \simeq N/M$  then  $M \geq N$  copies of  $|\psi\rangle$  are sufficient to perform, e.g., quantum teleportation of  $N$  qubits for  $N, M \gg 1$  (and similarly for other quantum communication protocols). Entanglement measures also exist for *mixed* states. The entanglement of formation of a bipartite state  $\chi$  (Bennett *et al.*, 1996b) is defined  $E(\chi) = \min_{\{(|\chi_i\rangle, p_i)\} \in \mathcal{E}(\chi)} \sum_i p_i S_N(|\chi_i\rangle)$ , where  $\mathcal{E}(\chi) = \{(|\chi_i\rangle, p_i) | \sum_i p_i |\chi_i\rangle\langle\chi_i| = \chi\}$  is the set of possible decompositions of the density matrix into ensembles of pure states. Therefore,  $E$  is the smallest averaged entanglement of any ensemble of pure states realizing  $\chi$ . In an operational sense,  $E(\chi)$  measures the number of EPR pairs (asymptotically, averaged over many copies) required to form one copy of the state  $\chi$ . A state with  $E > 0$  is entangled (a state with  $E = 1$ ) is maximally entangled and thus pure), and neither local operations nor classical communication (LOCC) between A and B can increase  $E$ .

Given an arbitrary mixed state of two qubits  $\chi$ , it is known that  $E(\chi)$  is a relatively complicated function of  $\chi$  (Wootters, 1998). In particular, it is in general certainly not a function of the singlet fidelity  $F_S = \langle\Psi_-|\chi|\Psi_- \rangle$  alone. For the subclass of spherically symmetric states, however, the entanglement only depends on  $F_S$ , i.e.,  $E(\chi) = E(F_S)$ . These states, known as Werner states (Werner, 1989), have the form

$$\rho_F = F_S |\Psi_- \rangle \langle \Psi_-| + \frac{1 - F_S}{3} (|\Psi_+ \rangle \langle \Psi_+| + |\Phi_- \rangle \langle \Phi_-| + |\Phi_+ \rangle \langle \Phi_+|). \quad (28)$$

There is an explicit analytic expression for the entanglement of formation of the Werner states (Bennett *et al.*, 1996b):

$$E(F_S) \equiv E(\rho_{F_S}) = \begin{cases} H_2 \left( 1/2 + \sqrt{F_S(1 - F_S)} \right) & \text{if } 1/2 < F_S \leq 1, \\ 0 & \text{if } 0 \leq F_S < 1/2, \end{cases} \quad (29)$$

where we have used the dyadic Shannon entropy  $H_2(x) = -x \log x - (1 - x) \log(1 - x)$ .

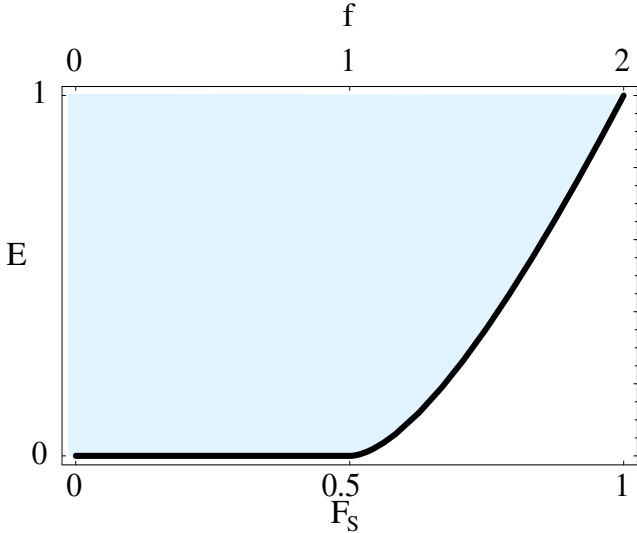


FIG. 6 Entanglement of formation  $E$  of the electron spins as a function of the singlet fidelity  $F_S$  and the reduced correlator  $f = S_{33}/2eIT(1 - T) = 2F_S$ . The points on the curve represent the exact relation for Werner states, the shaded (blue) area above the curve represents general states, for which the curve is a lower bound of  $E$ . Possible values of  $E$  and  $f$  (or  $F_S$ ) are in the shaded (blue) region.

Combining Eq. (29) with Eq. (27), one can express  $E(\rho_{F_S})$  in terms of the (reduced) shot noise power  $f$ . The relation between  $E(\rho_{F_S})$  and  $F_S$  (resp.,  $f$ ) is plotted in Fig. 6.

Using the expression for the entanglement of formation of Werner states, we can derive a lower bound on the entanglement of arbitrary mixed states  $\chi$  with the following argument. An arbitrary mixed state  $\chi$  can be transformed into a spherical symmetric state  $\rho_{F_S}$  with  $F_S = \langle \Psi_- | \chi | \Psi_- \rangle$  by a random bipartite rotation (“twirl”) (Bennett *et al.*, 1996a,b), i.e. by applying  $U \otimes U$  with a random  $U \in SU(2)$ . Because the twirl is a local (LOCC) operation, entanglement can only decrease (or remain constant) under the twirl,

$$E(F_S) \leq E(\chi). \quad (30)$$

As a consequence, the entanglement of formation  $E(F_S)$  of the associated Werner state (with same singlet fidelity  $F_S$ ) is a *lower bound* on  $E(\chi)$  (Fig. 6). If the noise power exceeds a certain value,  $f = 2F_S > 1$ , in the beam splitter setup Fig. 3 then we know that it must be due to entanglement between the electron spins injected into leads 1 and 2, i.e.,  $E(F_S) > 0$ .

## F. Use of spin-orbit coupling

The lower bound from Sec. II.E is useful if one is assessing a source that produces spin singlet entanglement. An extension to arbitrary entangled states is possible if a means of rotating the spin of the carriers in one of the ingoing arms of the beam splitter is available (Burkard and Loss, 2003; Egues *et al.*, 2002).

It has been proposed to use the Rashba spin orbit coupling in order to implement such single-spin rotations in one of the leads going into the beam splitter (Egues *et al.*, 2002). This analysis has been extended to up to two bands with both Rashba and Dresselhaus spin-orbit coupling present (Egues *et al.*, 2005).

We restrict ourselves here to the Rashba spin-orbit coupling and a single mode of the lead, to make the discussion as simple as possible. The Rashba spin-orbit coupling in, say, lead 1, has the effect of rotating the spin injected in lead 1 by some angle  $\theta_R$ . This can be taken into account by multiplying the rotation matrix

$$U_R = \begin{pmatrix} \cos \theta_R/2 & -\sin \theta_R/2 \\ \sin \theta_R/2 & \cos \theta_R/2 \end{pmatrix} \quad (31)$$

from the right to the scattering matrix blocks that involve lead 1,  $s_{31}^R = s_{31}U_R$  and  $s_{41}^R = s_{41}U_R$ . This rotates within the (entangled) singlet-triplet space, and yields the Fano factor

$$F = T(1 - T)(1 \mp \cos \theta_R \delta_{\varepsilon\varepsilon'}), \quad (32)$$

thus the classical inequality ( $F \leq 1$ ) can be violated for both the singlet and the entangled triplet by sweeping the Rashba angle  $\theta_R$ , while all unentangled triplet states still yield  $F \leq 1$ . Therefore, the Rashba rotation allows for the detection of entangled triplets in addition to the singlet. Similarly, spin rotations about an arbitrary axis allow the detection of all entangled states (in particular, all Bell states) with noise measurements.

## G. Backscattering

Imperfections in the leads and the beam splitter can lead to undesired scattering of electrons back into the same lead, or, e.g., from lead 1 to 2. Noisy injection from the entangler can be treated on the same footing as backscattering in the leads. In our discussion above, such backscattering processes has been neglected. Backscattering is a noise source which is unrelated to entanglement. Thus, it is important to ask whether there is a danger of a “false positive”, i.e., a noise signal that could be interpreted as entanglement although it really originates from backscattering. This problem has been analyzed for a symmetric beam splitter in (Burkard and Loss, 2003), and in more detail in (Egues *et al.*, 2005), where also the asymmetric backscattering of local Rashba spin-orbit interaction in one of the leads

was analyzed. The effect of inelastic backscattering (which we will not discuss here) has also been analyzed (San-Jose and Prada, 2006).

For symmetric backscattering with total backscattering probability  $R_B$ , one obtains (Burkard and Loss, 2003)

$$S_{33} = 2eI [2F_S(1 - R_B)T(1 - T) + R_B/2], \quad (33)$$

and similarly for the cross-correlations  $S_{34}$ , where the first term is the shot noise due to the (entangled) singlet fidelity  $F_S$  of the state, reduced by the backscattering factor  $1 - R_B$ , while the second term is the noise generated by the backscattering itself. As expected, Eq. (33) reduces to Eq. (14) for  $R_B = 0$ . As long as  $R_B > 1/2$ , one can still obtain a useful lower bound for entanglement (see Sec. II.E) even if  $R_B$  is not known precisely. If  $R_B$  is known, e.g., from measurements of the average current, then the backscattering effects can be taken into account and do not affect the quality of entanglement detection. Similar results apply for the backscattering due to spin-orbit coupling in one of the leads (Egues *et al.*, 2005).

## H. Bell's inequalities

Although they may be very challenging to do in practice (see above), direct tests of Bell's inequalities (Bell, 1966; Mermin, 1993) or related inequalities by Clauser and Horne (Clauser and Horne, 1974) with spin-entangled electrons using spin-sensitive detectors have been proposed by several authors (Kawabata, 2001; Maître *et al.*, 2000). In contrast to the charge detection in Secs. II.C and II.E this task involves the measurement of a spin current. Combinations of the Andreev entangler (see below) setup with a Bell test were studied in (Chtchelkatchev *et al.*, 2002; Samuelsson *et al.*, 2003). The possibility of a violation of the Clauser-Horne inequality in the full-counting statistics has been predicted in (Prada *et al.*, 2005). As an alternative to standard Bell tests, it has been proposed to use so-called entanglement witnesses (Blaauuboer and DiVincenzo, 2005).

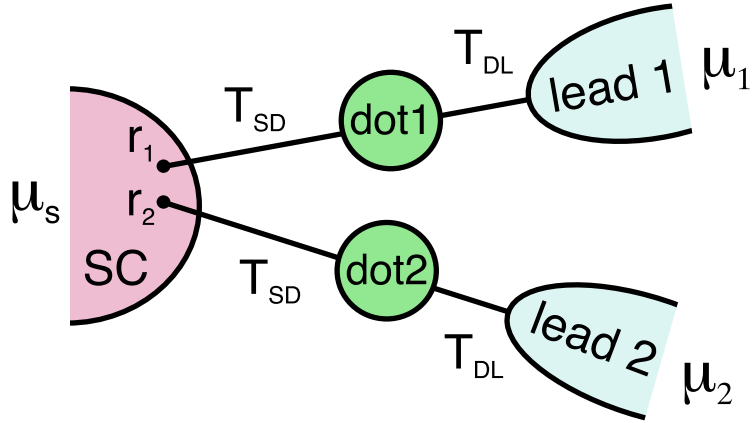


FIG. 7 Schematic of the Andreev entangler as proposed in (Recher *et al.*, 2001). Andreev tunneling takes place as follows: A Cooper pair in the superconductor (SC) is separated into two spin-entangled electrons which tunnel with amplitude  $T_{SD}$  from two points  $r_1, r_2$  of the SC onto the two quantum dots 1 and 2. The dots are coupled to normal leads 1 and 2 with tunneling amplitude  $T_{DL}$ . The entangler will be most efficient for asymmetric barriers,  $|T_{SD}|/|T_{DL}| \ll 1$ .

### III. PRODUCTION OF SPIN ENTANGLEMENT

#### A. Superconductor-normal junctions

The condensate in a conventional superconductor (SC) with s-wave pairing symmetry consists of a large number of Cooper pairs that are in the spin singlet state Eq. (1). A device that harnesses this large reservoir of entangled singlets has been proposed in (Recher *et al.*, 2001): It consists of a SC contact (at the chemical potential  $\mu_s$ ) from which quantum tunneling of single electrons to two quantum dots  $D_1$  and  $D_2$  is possible with a quantum amplitude  $T_{SD}$ . The quantum dots, in turn, are coupled with tunneling amplitude  $T_{DL}$  to the normal leads  $L_1$  and  $L_2$  (both at the chemical potential  $\mu_1 = \mu_2$ ), see Fig. 7.

The desired physical process for entanglement generation is Andreev tunneling where two electrons (one with spin up and another one with spin down) tunnel coherently through a normal barrier (Hekking *et al.*, 1993). At the same time, single-particle tunneling is suppressed by the presence of the intermediate quantum dots, forcing the two electrons from a Cooper pair to tunnel coherently into *separate* leads rather than both into the same lead. The double occupation of a quantum dot is suppressed by the Coulomb blockade

mechanism (Kouwenhoven *et al.*, 1997). The transport of entangled electrons from the SC the the quantum dots and from there to the normal leads can be controlled with an applied bias voltage  $\Delta\mu = \mu_S - \mu_l > 0$  ( $l = 1, 2$ ).

The parameter regime for the generation of spin-entangled electrons is discussed in (Recher *et al.*, 2001): The barriers of the quantum dots need to be asymmetric,  $|T_{SD}| \ll |T_{DL}|$ , the temperature must be sufficiently small,  $\Delta\mu > k_B T$ , and  $\Delta, U, \delta\epsilon > \Delta\mu > \gamma_l, k_B T$ , and  $\gamma_l > \gamma_S$ , where  $\Delta$  is the SC energy gap,  $\delta\epsilon$  is the single-level spacing of the dots, and  $\gamma_l = 2\pi\nu_l|T_{SD}|^2$  are the tunneling rates from lead  $l$  to the quantum dot (and vice versa). The quality of the device is characterized by the ratio between the current  $I_1$  of pairwise entangled electrons tunneling into different leads and the leakage current  $I_2$  of electron pairs that end up in the same lead (Recher *et al.*, 2001),

$$\frac{I_1}{I_2} = \frac{2\mathcal{E}^2}{\gamma^2} \left[ \frac{\sin(k_F\delta r)}{k_F\delta r} \right]^2 e^{-2\delta r/\pi\xi}, \quad (34)$$

$$\frac{1}{\mathcal{E}} = \frac{1}{\pi\Delta} + \frac{1}{U}. \quad (35)$$

Here,  $k_F$  denotes the Fermi wavevector,  $\gamma = \gamma_1 + \gamma_2$ , and  $\xi$  the SC coherence length.

The desired current  $I_1$  decreases exponentially with increasing distance  $\delta r = |\mathbf{r}_1 - \mathbf{r}_2|$  between the tunneling points on the SC, the scale given by the superconducting coherence length  $\xi$ . With  $\xi$  typically being on the order of  $\mu\text{m}$ , this does not pose severe restrictions for a conventional s-wave SC. In the important case  $0 \leq \delta r \sim \xi$  the suppression is only polynomial  $\propto 1/(k_F\delta r)^2$ , with  $k_F$  being the Fermi wavevector in the SC. One also observes that the effect of the quantum dots consists in the suppression factor  $(\gamma/\mathcal{E})^2$  for tunneling into the same lead. One therefore has to impose the additional condition  $k_F\delta r < \mathcal{E}/\gamma$ , which can be satisfied for small dots with  $\mathcal{E}/\gamma \approx 100$  and  $k_F^{-1} \approx 1 \text{ \AA}$ .

Electron entangler devices with a SC reservoir attached to normal leads have also been investigated in (Lesovik *et al.*, 2001; Prada and Sols, 2004; Sauret *et al.*, 2004). The presence of voltage noise on the two quantum dots can lead to a reduction of the ratio Eq. (34), as analyzed in (Dupont and Hur, 2006).

Shot noise and conductance measurements have been achieved in a quasi-ballistic SC-normal beam-splitter junction (Choi *et al.*, 2005). Moreover, transport properties of structures with a SC lead attached to normal leads have been studied experimentally (Russo *et al.*, 2005).



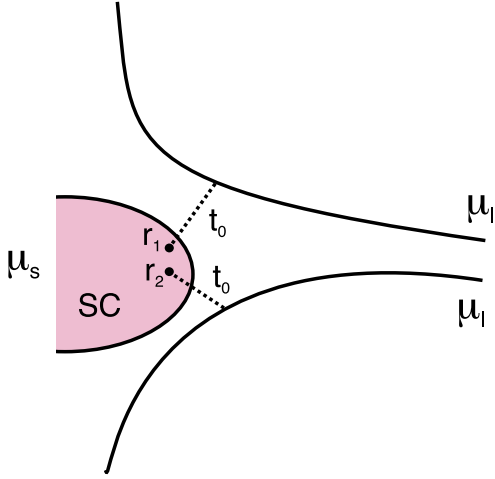


FIG. 8 The entangler as proposed in (Recher and Loss, 2002a,b), with a superconductor (SC) tunnel-coupled to two one-dimensional wires at positions  $\mathbf{r}_1$  and  $\mathbf{r}_2$  on the SC with tunneling amplitude  $t_0$ .

## B. Superconductor-Luttinger liquid junctions

The production of electron spin entanglement requires interaction between the electrons; in the case discussed in the previous Sec. III.A, the repulsive Coulomb interaction in the quantum dots attached to the SC reservoir is used to separate the two entangled electrons. Alternatively, a resistive lead where the dynamical Coulomb blockade effect helps to separate the electron pair has been proposed (Recher and Loss, 2003).

A strongly interacting electron system in one spatial dimension can be described as a Luttinger liquid (Tsvetlik, 2003). A Luttinger liquid opens another possibility to separate entangled electrons from a SC (Bena *et al.*, 2002; Recher and Loss, 2002a,b). Physical systems with Luttinger liquid behavior are e.g. metallic carbon nanotubes (Egger and Gogolin, 1997; Kane *et al.*, 1997). The setup studied theoretically in (Recher and Loss, 2002a,b) is composed of two separate one-dimensional conductors (e.g., carbon nanotubes), each forming a Luttinger liquid, which are tunnel-coupled (at a point far from their ends) to a SC, see Fig. 8. The two wires are assumed to be sufficiently separated, such that interactions between carriers in different wires can be neglected.

The fundamental excitations of a Luttinger liquid (if backscattering is absent) are long-wavelength charge and spin density waves propagating with velocities  $u_\rho = v_F/K_\rho$  (charge) and  $u_\sigma = v_F$  (spin) (Schulz, 1990), with  $v_F$  the Fermi velocity and  $K_\rho < 1$  for an interacting system. The tunneling of electrons from the SC to the one-dimensional (Luttinger liquid) wires is modeled by the Hamiltonian

$$H_T = t_0 \sum_{ns} \psi_{ns}^\dagger \Psi_s(\mathbf{r}_n) + \text{H.c.}, \quad (36)$$

where  $\Psi_s(\mathbf{r}_n)$  is the annihilation (field) operator for an electron with spin  $s$  at the location  $\mathbf{r}_n$  in the SC nearest to the one-dimensional wire  $n = 1, 2$ , and  $\psi_{ns}^\dagger$  is the operator that creates an electron at the coordinate  $x_n$  in the wire  $n$ . Applying a bias  $\mu = \mu_S - \mu_l$  between the SC (with chemical potential  $\mu_S$ ) and the leads ( $\mu_l$ ) induces the flow of a stationary current of pairwise spin-entangled from the SC to the one-dimensional wires.

Similar to the case of the Andreev entangler with attached quantum dots, discussed in Sec. III.A above, the performance of this device can be quantified by the ratio between the two competing currents,  $I_1$  for electrons tunneling into separate leads, thus contributing to entanglement between the remote parts of the system, and  $I_2$  for electrons tunneling into the same lead, thus not contributing to entanglement. From a T-matrix calculation (Recher and Loss, 2002a,b), one obtains in leading order in  $\mu/\Delta$ , where  $\Delta$  denotes the SC excitation gap, and at zero temperature,

$$I_1 = \frac{I_1^0}{\Gamma(2\gamma_\rho + 2)} \frac{v_F}{u_\rho} \left[ \frac{2\Lambda\mu}{u_\rho} \right]^{2\gamma_\rho}, \quad (37)$$

$$I_1^0 = 4\pi e \gamma^2 \mu \frac{\sin^2(k_F \delta r)}{(k_F \delta r)^2} e^{-2\delta r/\pi\xi}, \quad (38)$$

$$I_2 = I_1(\delta r \rightarrow 0) \sum_{b=\pm 1} A_b \left( \frac{2\mu}{\Delta} \right)^{2\gamma_{\rho b}}, \quad (39)$$

where  $\Gamma$  is the Gamma function,  $\Lambda$  a short distance cut-off on the order of the lattice spacing in the Luttinger liquid,  $\gamma = 2\pi\nu_S\nu_l|t_0|^2$  the probability per spin to tunnel from the SC to the one-dimensional leads,  $\nu_S$  and  $\nu_l$  the energy DOS per spin for the SC and the one-dimensional leads at the chemical potentials  $\mu_S$  and  $\mu_l$ , respectively, and  $\delta r$  the separation between the tunneling points on the SC. The constant  $A_b$  is of order one and does not depend on the interaction strength. Furthermore, we have used the definitions  $\gamma_{\rho+} = \gamma_\rho$  and  $\gamma_{\rho-} = \gamma_{\rho+} + (1 - K_\rho)/2 > \gamma_{\rho+}$ . Note that in Eq. (39), the current  $I_1$  needs to be evaluated at  $\delta r = 0$ . In the non-interacting limit,  $I_2 = I_1 = I_1^0$  is obtained by putting  $\gamma_\rho = \gamma_{\rho b} = 0$ , and  $u_\rho = v_F$ .

In order to obtain a finite measurable current, the coherence length  $\xi$  of the Cooper pairs should exceed  $\delta r$  (as in Sec. III.A for the Andreev entangler). It has been argued that the suppression of the current by  $1/(k_F \delta r)^2$  can be considerably reduced by using low-dimensional SCs (Recher and Loss, 2002a,b). The undesired injection of two electrons into the same lead (current  $I_2$ ) is suppressed compared to  $I_1$  by a factor of  $(2\mu/\Delta)^{2\gamma_{\rho+}}$ , where  $\gamma_{\rho+} = \gamma_\rho$ , if the two electrons are injected into the same direction (left or right movers), or

by  $(2\mu/\Delta)^{2\gamma_{\rho-}}$  if they propagate in different directions. The first scenario (same direction) is the more likely one since  $\gamma_{\rho-} > \gamma_{\rho+}$ . The suppression of  $I_2$  by  $1/\Delta$  is due to the two-particle correlations in the Luttinger liquid when the electrons tunnel into the same lead, similar to the Coulomb blockade effect for tunneling into quantum dots in the previous Sec. III.A. The delay time between the two electrons from the same Cooper pair is controlled by the inverse SC gap  $\Delta^{-1}$ , i.e., if  $\Delta$  becomes larger, the electrons arrive within a shorter time interval, thus increasing the correlations and further suppressing the unwanted  $I_2$ . Increasing the bias  $\mu$  has the opposite effect, since it opens up more available states into which the electron can tunnel, and therefore the effect of the SC gap  $\Delta$  is mitigated.

Noise correlations in the current carried by the entangled electrons emitted by a carbon nanotube–SC entangler are studied in (Bouchiat *et al.*, 2003).

### C. Quantum dots coupled to normal leads

The Coulomb interaction between electrons in a quantum dot has also been suggested as the main mechanism in electron spin entanglers with normal (as opposed to SC) leads. An entangler comprising a single quantum dot attached to special leads with a very narrow bandwidth (Oliver *et al.*, 2002) or with three coupled quantum dots (Saraga and Loss, 2003) coupled to ordinary leads have been analyzed. The idea behind both proposals is to extract the singlet ground state of a single quantum dot occupied by two electrons by moving the two electrons into two separate leads. In both proposals, the separation is enhanced due to two-particle energy conservation. Different ideas using double-dot turnstile devices with time-dependent barriers were followed in (Blauboer and DiVincenzo, 2005; Hu and Das Sarma, 2004).

### D. Coulomb scattering in a 2D electron system

Motivated by scanning probe imaging and control of electron flow in a two-dimensional electron system in a semiconductor heterostructure (Topinka *et al.*, 2000, 2001), it has been proposed to use this technique to generate electron spin entanglement by controlling Coulomb scattering in a interacting 2D electron system (Saraga *et al.*, 2004, 2005). For a scattering angle of  $\pi/2$ , constructive two-particle interference is expected to lead to an

enhancement of the spin-singlet scattering probability, and at the same time, a reduction of the triplet scattering. These scattering amplitudes (and probabilities) have been obtained using the Bethe-Salpeter equation for small  $r_s$ , which in turn allowed for an estimate of the achievable current of spin-entangled electrons (Saraga *et al.*, 2004, 2005).

### E. Other spin entangler proposals

In (Costa and Bose, 2001), the use of a magnetic impurity in a special beam-splitter geometry was proposed for the purpose of generating spin entanglement between ballistic electrons in a two-dimensional electron system. The process where two magnetic impurities become entangled via electron scattering has been described more recently (Costa *et al.*, 2006).

The generation of entanglement using two-particle interference in combination with which-way detection (charge detection) has been discussed in (Bose and Home, 2002).

The use of a sole carbon nanotube to create spin entanglement between a localized and an itinerant electron has been suggested in (Gunlycke *et al.*, 2006).

Entanglement between electrons subject to the spin-orbit interaction in a quantum dot, in the absence of interaction, has been discussed in (Frustaglia *et al.*, 2006).

## IV. TRANSPORT OF ENTANGLED ELECTRONS

An electron spin qubit does not travel “on its own”—it is always attached to the electron’s charge. This is an enormous advantage for many reasons, one being that spin information can be converted into charge information which then allows sensitive read-out (Loss and DiVincenzo, 1998). Another advantage, of interest in the present context, is that the charge responds to externally applied fields and therefore electron spin qubits can in principle be transported in an electric conductor.

This has prompted the question whether a pair of entangled electron spins could be produced in one location on a semiconductor structure and subsequently distributed over some distance on-chip, to be consumed later for some quantum information task (see Sec. I.A). Such transport has certainly reached quite an advanced level for photon qubits, reaching distances of kilometers (Gisin *et al.*, 2002). Even for modest distances, perhaps microme-

ters, within, e.g., a semiconductor structure, this is not straight-forward for electrons. An electron that is injected into a metallic wire becomes immersed into a sea of other electrons that (i) are indistinguishable from the injected electron, and (ii) interact with all other electrons, including the injected one. Here, we report on the theoretical discussion regarding the stability of spin entanglement in an interacting many-electron system (Burkard *et al.*, 2000; DiVincenzo and Loss, 1999). To anticipate the main results, it turns out that the indistinguishability of particles is harmless for spin entanglement, whereas Coulomb interactions do affect entanglement, but only to some extent because the electron-electron interactions are typically screened (Mahan, 1993). As discussed in more detail below, an electron being added to the a metallic wire in the orbital state  $q$  will be “dressed” by the interactions on a very short time scale (inverse plasma frequency). The resulting state has a quasiparticle weight in state  $q$  which is renormalized by a factor  $z_f$  with  $0 \leq z_q \leq 1$ . The weight  $z_q$  quantifies how likely it is to find an electron in the original state  $q$ , while  $1 - z_q$  is the part that is distributed among all the other states.

We can describe the time evolution of the entangled triplet or singlet states in the interacting many-electron system by introducing the 2-particle Green’s function

$$G^{t/s}(\mathbf{12}, \mathbf{34}; t) = \left\langle \psi_{\mathbf{12}}^{t/s}, t | \psi_{\mathbf{34}}^{t/s} \right\rangle, \quad (40)$$

where we use the second-quantized notation introduced in Eq. (8) above. The singlet/triplet Green’s function defined in Eq. (40) above can be expressed in terms of the standard two-particle Green’s function (Mahan, 1993)  $G(12, 34; t)$  by

$$G^{t/s}(\mathbf{12}, \mathbf{34}; t) = -\frac{1}{2} \sum_{\sigma} [G(1\bar{2}, 3\bar{4}; t) \pm G(1\bar{2}, \bar{3}4; t)], \quad (41)$$

where  $n = (\mathbf{n}, \sigma)$  and  $\bar{n} = (\mathbf{n}, -\sigma)$ . The  $+$  sign stands for the triplet (t), the  $-$  sign for the singlet (s), Green’s function. If at time  $t = 0$ , a spin triplet (singlet) state is prepared, then we can define the fidelity of transmission as the probability for finding a triplet (singlet) after time  $t$ ,

$$P(t) = |G^{t/s}(\mathbf{12}, \mathbf{12}; t)|^2. \quad (42)$$

To calculate the fidelity Eq. (42), we can therefore use Eq. (41) to reduce the problem to that of calculating the (standard) two-particle Green’s function

$$G(12, 34; t) = -\left\langle T a_1(t) a_2(t) a_3^\dagger a_4^\dagger \right\rangle \quad (43)$$

for a time- and spin-independent Hamiltonian,  $H = H_0 + \sum_{i<j} V_{ij}$ , where  $H_0$  describes the free motion of  $N$  electrons, and  $V_{ij}$  is the bare Coulomb interaction between electrons  $i$  and  $j$ ,  $\langle \dots \rangle$  denotes the zero-temperature expectation value, and  $T$  is the time-ordering operator. In the case where the leads are sufficiently separated, the vertex part in  $G(12, 34; t)$  vanishes, and thus the two-particle Green's function can be expressed in terms of interacting single-particle Green's functions  $G(\mathbf{n}, t)$  via

$$G(12, 34; t) = G(13, t)G(24, t) - G(14, t)G(23, t), \quad (44)$$

where ( $l = 1, 2$ )

$$G(\mathbf{n}, t) = -i\langle \psi_0 | T a_{\mathbf{n}}(t) a_{\mathbf{n}}^\dagger | \psi_0 \rangle \equiv G_l(\mathbf{q}, t). \quad (45)$$

For the singlet/triplet Green's functions, this leads, with Eq. (41), to

$$G^{t/s}(\mathbf{12}, \mathbf{34}; t) = -G(\mathbf{1}, t)G(\mathbf{2}, t)[\delta_{\mathbf{13}}\delta_{\mathbf{24}} \mp \delta_{\mathbf{14}}\delta_{\mathbf{23}}]. \quad (46)$$

At  $t = 0$  (or as long as interactions are absent) one finds  $G(\mathbf{n}, t) = -i$  and  $G^{t/s} = \delta_{\mathbf{13}}\delta_{\mathbf{24}} \mp \delta_{\mathbf{14}}\delta_{\mathbf{23}}$ , the fidelity remains  $P = 1$ . Under the influence of interactions and for times  $0 \leq t \lesssim 1/\Gamma_q$  shorter than the quasiparticle lifetime  $1/\Gamma_q$ , one can use the standard result for particle energies  $\epsilon_q = q^2/2m$  near the Fermi energy  $\epsilon_F$  (Mahan, 1993),

$$G_{1,2}(\mathbf{q}, t) \approx -iz_q \theta(\epsilon_q - \epsilon_F) e^{-i\epsilon_q t - \Gamma_q t}. \quad (47)$$

In a two-dimensional electron system (2DES), e.g. in a GaAs heterostructure, one finds  $\Gamma_q \propto (\epsilon_q - \epsilon_F)^2 \log(\epsilon_q - \epsilon_F)$  (Giuliani and Quinn, 1982) using the random phase approximation (RPA) to take into account the screening of the Coulomb interaction (Mahan, 1993). It remains to evaluate the quasiparticle weight at the Fermi surface,

$$z_F = \left( 1 - \frac{\partial}{\partial \omega} \text{Re} \Sigma_{\text{ret}}(k_F, \omega) \right)^{-1} \Big|_{\omega=0}, \quad (48)$$

where  $\Sigma_{\text{ret}}(q, \omega)$  is the retarded irreducible self-energy. The fidelity can then be expressed through  $z_F$  as

$$P = z_F^4. \quad (49)$$

This can be seen by evaluating the two-particle Green's function for momenta  $\mathbf{q}$  near the Fermi surface, assuming that the two leads that carry the two entangled particles are identical ( $G_1 = G_2$ ). One finds  $|G^{t/s}(\mathbf{12}, \mathbf{34}; t)|^2 = z_F^4 |\delta_{\mathbf{13}}\delta_{\mathbf{24}} \mp \delta_{\mathbf{14}}\delta_{\mathbf{23}}|^2$ , for sufficiently short times,  $0 < t \lesssim 1/\Gamma_q$ .

Finally, in order to evaluate the quasiparticle weight factor, Eq. (50), we need the the irreducible self-energy  $\Sigma_{\text{ret}}$ . For a two-dimensional electron system (2DES), this quantity has been evaluated explicitly in leading order of the interaction parameter  $r_s = 1/k_F a_B$ , where  $a_B = \epsilon_0 \hbar^2 / m e^2$  is the Bohr radius, in (Burkard *et al.*, 2000; DiVincenzo and Loss, 1999), with the result

$$z_F = \frac{1}{1 + r_s (1/2 + 1/\pi)}. \quad (50)$$

This result has been extended to include corrections due to the Rashba spin-orbit interaction (Saraga and Loss, 2005) and finite temperatures (Galitski and Sarma, 2004). In a standard GaAs 2DES, one can estimate  $a_B = 10.3 \text{ nm}$  and  $r_s = 0.614$ , which yields a quasiparticle weight of  $z_F = 0.665$ . Numerical evaluation of the RPA self-energy, summing up all orders of  $r_s$  within this approximation, yield the more accurate result  $z_F = 0.691$ . Substituting  $z_F$  back into Eq. (49), we obtain approximately  $P \approx 0.2$ . For larger electron density, i.e., smaller  $r_s$ , one can expect  $P$  to be closer to one. It also needs to be stressed that  $P$  is a fidelity without postselection. Typically, it is sufficient to count only the fidelity of the postselected singlet pairs, i.e., those that can successfully be retrieved from the Fermi sea. This postselected fidelity is not affected by the (spin-independent) Coulomb interaction at all, i.e.,  $P_{\text{postsel}} = 1$ , provided that spin-scattering effects are negligible. The degree to which spin-scattering events are really negligible can be quantified from experiments that measure the spin coherence length (Awschalom and Kikkawa, 1999; Kikkawa and Awschalom, 1998; Kikkawa *et al.*, 1997). In these experiments, it was found that the spin coherence length can exceed  $100 \mu\text{m}$  in in GaAs 2DES's.

## References

- Aspect, A., J. Dalibard, and G. Roger, 1982, Phys. Rev. Lett. **49**, 1804.
- Averin, D. V., and Y. V. Nazarov, 1992, in *Single Charge Tunneling*, edited by H. Grabert and M. H. Devoret (Plenum Press, New York), volume 294 of *NATO ASI Series B: Physics*.
- Awschalom, D. D., and J. M. Kikkawa, 1999, Phys. Today **52**(6), 33.
- Beenakker, C. W. J., 2006 (IOS Press, Amsterdam), volume 162 of *Proc. Int. School Phys. E. Fermi*, cond-mat/9906071.
- Bell, J. S., 1966, Rev. Mod. Phys. **38**, 447.
- Bena, C., S. Vishveshwara, L. Balents, and M. P. A. Fisher, 2002, Phys. Rev. Lett. **89**, 037901.

- Bennett, C. H., G. Brassard, C. Crépeau, R. Jozsa, A. Peres, and W. K. Wootters, 1993, Phys. Rev. Lett. **70**, 1895.
- Bennett, C. H., G. Brassard, S. Popescu, B. Schumacher, J. A. Smolin, and W. K. Wootters, 1996a, Phys. Rev. Lett. **76**, 722.
- Bennett, C. H., and D. P. DiVincenzo, 2000, Nature **404**, 247.
- Bennett, C. H., D. P. DiVincenzo, J. A. Smolin, and W. K. Wootters, 1996b, Phys. Rev. A **54**, 3824.
- Bennett, C. H., and S. J. Wiesner, 1992, Phys. Rev. Lett. **69**, 2881.
- Blaauboer, M., and D. P. DiVincenzo, 2005, Phys. Rev. Lett. **95**(16), 160402.
- Blanter, Y. M., and M. Büttiker, 2000, Phys. Rep. **336**, 1.
- Börlin, J., W. Belzig, and C. Bruder, 2002, Phys. Rev. Lett. **88**, 197001.
- Boschi, D., S. Branca, F. De Martini, L. Hardy, and S. Popescu, 1998, Phys. Rev. Lett. **80**, 1121.
- Bose, S., and D. Home, 2002, Physical Review Letters **88**(5), 050401.
- Bouchiat, V., N. Chtchelkatchev, D. Feinberg, G. B. Lesovik, T. Martin, and J. Torrès, 2003, Nanotechnology **14**(1), 77.
- Bouwmeester, D., J.-W. Pan, K. Mattle, M. Eibl, H. Weinfurter, and A. Zeilinger, 1997, Nature **390**, 575.
- Burkard, G., and D. Loss, 2003, Phys. Rev. Lett. **91**, 087903.
- Burkard, G., D. Loss, and D. P. DiVincenzo, 1999, Phys. Rev. B **59**, 2070.
- Burkard, G., D. Loss, and E. V. Sukhorukov, 2000, Phys. Rev. B **61**, R16303, cond-mat/9906071.
- Büttiker, M., 1990, Phys. Rev. Lett. **65**, 2901.
- Büttiker, M., 1992, Phys. Rev. B **46**, 12485.
- Cerletti, V., O. Gywat, and D. Loss, 2005, Phys. Rev. B **72**(11), 115316.
- Chen, Y., and R. A. Webb, 2006, Phys. Rev. Lett. **97**, 066604.
- Choi, B.-R., A. E. Hansen, T. Kontos, C. Hoffmann, S. Oberholzer, W. Belzig, C. Schönenberger, T. Akazaki, and H. Takayanagi, 2005, Phys. Rev. B **72**(2), 024501.
- Choi, M.-S., C. Bruder, and D. Loss, 2000, Phys. Rev. B **62**, 13569.
- Chtchelkatchev, N. M., G. Blatter, G. B. Lesovik, and T. Martin, 2002, Phys. Rev. B **66**, 161320.
- Clauser, J. F., and M. A. Horne, 1974, Phys. Rev. D **10**, 526.
- Costa, A. T., and S. Bose, 2001, Phys. Rev. Lett. **87**(27), 277901.
- Costa, A. T., S. Bose, and Y. Omar, 2006, Phys. Rev. Lett. **96**(23), 230501.



- Devetak, I., A. W. Harrow, and A. Winter, 2004, *Phys. Rev. Lett.* **93**(23), 230504.
- Di Lorenzo, A., and Y. V. Nazarov, 2005, *Phys. Rev. Lett.* **94**(21), 210601.
- DiVincenzo, D. P., and D. Loss, 1999, *J. Mag. Magn. Matl.* **200**, 202.
- Dowling, M. R., A. C. Doherty, and H. M. Wiseman, 2006, *Phys. Rev. A* **73**(5), 052323.
- Dupont, É., and K. L. Hur, 2006, *Phys. Rev. B* **73**, 045325.
- Egger, R., and A. Gogolin, 1997, *Phys. Rev. Lett.* **79**, 5082.
- Egues, J. C., G. Burkard, and D. Loss, 2002, *Phys. Rev. Lett.* **89**, 176401.
- Egues, J. C., G. Burkard, D. S. Saraga, J. Schliemann, and D. Loss, 2005, *Phys. Rev. B* **72**, 235326.
- Egues, J. C., P. Recher, D. S. Saraga, V. N. Golovach, G. Burkard, E. V. Sukhorukov, and D. Loss, 2003, in *Quantum Noise in Mesoscopic Physics* (Kluwer, The Netherlands), volume 97 of *NATO Science Series*, pp. 241–274, cond-mat/0210498.
- Einstein, A., B. Podolsky, and N. Rosen, 1935, *Phys. Rev.* **47**, 777.
- Ekert, A. K., 1991, *Phys. Rev. Lett.* **67**, 661.
- Faoro, L., F. Taddei, and R. Fazio, 2004, *Phys. Rev. B* **69**, 125326.
- Frustaglia, D., S. Montangero, and R. Fazio, 2006, *Phys. Rev. B* **74**(16), 165326.
- Galitski, V. M., and S. D. Sarma, 2004, *Phys. Rev. B* **70**(3), 035111.
- Giovannetti, V., D. Frustaglia, F. Taddei, and R. Fazio, 2006, *Phys. Rev. B* **74**(11), 115315.
- Gisin, N., G. Ribordy, W. Tittel, and H. Zbinden, 2002, *Rev. Mod. Phys.* **74**, 145.
- Giuliani, G. F., and J. J. Quinn, 1982, *Phys. Rev. B* **26**, 4421.
- Gunlycke, D., J. H. Jefferson, T. Rejec, A. Ramsak, D. G. Pettifor, and G. A. D. Briggs, 2006, *Journal of Physics: Condensed Matter* **18**(21), S851.
- Gywat, O., G. Burkard, and D. Loss, 2002, *Phys. Rev. B* **65**, 205329.
- Hanbury Brown, R., and R. Q. Twiss, 1956, *Nature* **177**, 27.
- Hanson, R., L. P. Kouwenhoven, J. R. Petta, S. Tarucha, and L. M. K. Vandersypen, 2006, Spins in few-electron quantum dots, submitted to *Rev. Mod. Phys.* (cond-mat/0610433).
- Hekking, F. W. J., L. I. Glazman, K. A. Matveev, and R. I. Shekhter, 1993, *Phys. Rev. Lett.* **70**, 4138.
- Henny, M., S. Oberholzer, C. Strunk, T. Heinzel, K. Ensslin, M. Holland, and C. Schönberger, 1999, *Science* **284**, 296.
- Hohenester, U., 2002, *Phys. Rev. B* **66**, 245323.
- Hong, C. K., Z. Y. Ou, and L. Mandel, 1987, *Phys. Rev. Lett.* **59**(18), 2044.

- Hu, X., and S. Das Sarma, 2004, *Phys. Rev. B* **69**, 115312.
- Kane, C., L. Balents, and M. Fisher, 1997, *Phys. Rev. Lett.* **79**, 5086.
- Kawabata, S., 2001, *J. Phys. Soc. Jpn.* **70**, 1210.
- Khlus, V. A., 1987, *Zh. Eksp. Teor. Fiz.* **93**, 2179.
- Kikkawa, J. M., and D. D. Awschalom, 1998, *Phys. Rev. Lett.* **80**, 4313.
- Kikkawa, J. M., I. P. Smorchkova, N. Samarth, and D. D. Awschalom, 1997, *Science* **277**, 1284.
- Kouwenhoven, L. P., G. Schön, and L. L. Sohn (eds.), 1997, *Mesoscopic Electron Transport*, volume 345 of *NATO ASI Series E* (Kluwer Academic Publishers, Dordrecht).
- Landauer, R., 1989, *Physica D* **38**, 226.
- Lesovik, G., T. Martin, and G. Blatter, 2001, *Eur. Phys. J. B* **24**, 287.
- Lesovik, G. B., 1989, *Pis'ma Zh. Eksp. Teor. Fiz.* **49**, 513.
- Lim, Y. L., and A. Beige, 2005, *New J. Phys.* **7**, 155.
- Liu, R. C., B. Odom, Y. Yamamoto, and S. Tarucha, 1998, *Nature* **391**, 263.
- Loss, D., and D. P. DiVincenzo, 1998, *Phys. Rev. A* **57**(1), 120.
- Loss, D., and E. V. Sukhorukov, 2000, *Phys. Rev. Lett.* **84**, 1035.
- Loudon, R., 1998, *Phys. Rev. A* **58**, 4904.
- Mahan, G. D., 1993, *Many Particle Physics* (Plenum, New York), 2nd edition.
- Maitre, X., W. D. Oliver, and Y. Yamamoto, 2000, *Physica E* **6**, 301.
- Martin, T., and R. Landauer, 1992, *Phys. Rev. B* **45**, 1742.
- Mattle, K., H. Weinfurter, P. G. Kwiat, and A. Zeilinger, 1996, *Phys. Rev. Lett.* **76**, 4656.
- Mermin, N. D., 1993, *Rev. Mod. Phys.* **65**, 803.
- Oberholzer, S., E. Bieri, C. Schonenberger, M. Giovannini, and J. Faist, 2006, *Physical Review Letters* **96**(4), 046804.
- Oliver, W. D., J. Kim, R. C. Liu, and Y. Yamamoto, 1999, *Science* **284**, 299.
- Oliver, W. D., F. Yamaguchi, and Y. Yamamoto, 2002, *Phys. Rev. Lett.* **88**, 037901.
- Prada, E., and F. Sols, 2004, *Eur. Phys. J. B* **40**, 379.
- Prada, E., F. Taddei, and R. Fazio, 2005, *Phys. Rev. B* **72**, 125333.
- Prinz, G. A., 1998, *Science* **282**, 1660.
- Recher, P., and D. Loss, 2002a, *Journal of Superconductivity and Novel Magnetism* **15**, 49, cond-mat/0202102.
- Recher, P., and D. Loss, 2002b, *Phys. Rev. B* **65**, 165327.

- Recher, P., and D. Loss, 2003, Phys. Rev. Lett. **91**, 267003.
- Recher, P., E. V. Sukhorukov, and D. Loss, 2001, Phys. Rev. B **63**, 165314.
- Russo, S., M. Kroug, T. M. Klapwijk, and A. F. Morpurgo, 2005, Phys. Rev. Lett. **95**(2), 027002.
- Samuelsson, P., E. V. Sukhorukov, and M. Büttiker, 2003, Phys. Rev. Lett. **91**, 157002.
- Samuelsson, P., E. V. Sukhorukov, and M. Büttiker, 2004, Phys. Rev. B **70**, 115330.
- San-Jose, P., and E. Prada, 2006, Phys. Rev. B **74**(4), 045305.
- Saraga, D. S., B. L. Altshuler, D. Loss, and R. M. Westervelt, 2004, Phys. Rev. Lett. **92**, 246803.
- Saraga, D. S., B. L. Altshuler, D. Loss, and R. M. Westervelt, 2005, Phys. Rev. B **71**, 045338.
- Saraga, D. S., and D. Loss, 2003, Phys. Rev. Lett. **90**, 166803.
- Saraga, D. S., and D. Loss, 2005, Phys. Rev. B **72**(19), 195319.
- Sauret, O., D. Feinberg, and T. Martin, 2004, Phys. Rev. B **70**(24), 245313.
- Schliemann, J., J. I. Cirac, M. Kus, M. Lewenstein, and D. Loss, 2001a, Phys. Rev. A **64**, 022303.
- Schliemann, J., D. Loss, and A. H. MacDonald, 2001b, Phys. Rev. B **63**, 085311.
- Schrödinger, E., 1935, Die Naturwissenschaften **23**, 807.
- Schulz, H. J., 1990, Phys. Rev. Lett. **64**, 2831.
- Sukhorukov, E. V., G. Burkard, and D. Loss, 2001, Phys. Rev. B **63**, 125315.
- Taddei, F., L. Faoro, E. Prada, and R. Fazio, 2005, New J. Phys. **7**, 183.
- Taddei, F., and R. Fazio, 2002, Phys. Rev. B **65**, 075317.
- Taylor, J. M., W. Dur, P. Zoller, A. Yacoby, C. M. Marcus, and M. D. Lukin, 2005, Phys. Rev. Lett. **94**, 236803.
- Topinka, M. A., B. J. LeRoy, S. E. J. Shaw, E. J. Heller, R. M. Westervelt, K. D. Maranowski, and A. C. Gossard, 2000, Science **289**, 2323.
- Topinka, M. A., B. J. Leroy, R. M. Westervelt, S. E. J. Shaw, R. Fleischmann, E. J. Heller, K. D. Maranowski, and A. C. Gossard, 2001, Nature **410**, 183.
- Torrès, J., and T. Martin, 1999, Eur. Phys. J. B **12**, 319.
- Tsvetlik, A. M., 2003, *Quantum Field Theory in Condensed Matter Physics* (Cambridge University Press), 2nd edition.
- Werner, R. F., 1989, Phys. Rev. A **40**, 4277.
- Wiseman, H. M., and J. A. Vaccaro, 2003, Phys. Rev. Lett. **91**(9), 097902.
- Wootters, W. K., 1998, Phys. Rev. Lett. **80**, 2245.